La Société Savante
de l'Aéronautique et de l'Espace

49th International Symposium of Applied Aerodynamics
Lille, 24-25-26 March 2014

FP05-2014-paquet

Formulation of Aerodynamic Forces on Helicopters in Non Uniform Flow with Scale Model Tests : Ground Effects

Lille, France, 24-25-26 MARCH 2014

Jean-Bernard Paquet [(1)], Jean-Paul Bourez [(1)], Stéphane Morgand [(1)]

[(1)] ONERA – the French Aerospace Lab – F-59045 Lille, France
jean-bernard.paquet@onera.fr, jean-paul.bourez@onera.fr, stephanemorgand@neuf.fr

INTRODUCTION

The simulation of helicopter recovery on a frigate is a very complex problem due to the non uniform flow around the frigate deck and the aeroelastic characteristics of the rotor. Small scale tests with helicopters are generally not in complete similarity and might be expensive. The number of state variables influencing the aerodynamic forces are too numerous so it is not possible to characterize all the configurations. So these tests with a small scale radio controlled helicopter attached to a balance and not flying are done as an attempt to measure the differences on the aerodynamic torque due to the non uniform flow around a frigate. To validate the experimental procedure, measurements are done with and without a ground, and flow visualizations are carried out. The forces measurements of the ground effects correspond to known results and the trajectories of vortices shed at the blade tips are extracted from the visualizations.

1. OBJECTIVES

The final objective being the formulation of the aerodynamic forces on an helicopter during the last phase of its recovery on a frigate deck, it is necessary to distinguish between the different aspects and to verify the validity of the hypotheses done for the formulation. A review of the rotor-ship aerodynamic interface modelling was presented in [9]. Lot of experiments and computations were done to characterize the flow around a frigate alone and without any movement of its [2][4][5][6][7]. The frequency of its movement is relatively low when compared to the frequencies of the blade and even to the natural frequencies of the helicopter in flight. So a quasi-static hypothesis is always done on the effect of the ship movement. For a first approach and particularly to simplify the problem, the interaction between the flows around the frigate and the helicopter is not taken into account. The characterization of the flow around the frigate alone gives the flow field in which the helicopter flies.

The previous assumption is not actually correct, the interactions between the flow around the frigate and the flow induced by the rotor are strong. The flow generated by a rotor near a frigate deck changes the structure of the flow around the frigate alone. The visualization of the flow (Fig. 1) shows that dowstream of the deck of a frigate the rotor changes the recirculation zone. Instead of a recirculation zone with a reattachment point on the deck at about three times the deck height, the blades shed vortices in front of it and a short recirculation zone appears in front of the helicopter. Of course the similarity conditions are not sufficient to extrapolate these results from tests with a small scale model dowstream of a step. Nevertheless we do the hypothesis that it is sufficient to consider a rotor in an upstream non uniform flow without taking into consideration the unsteady flow on the rotating blades in the wake of the ship.



Figure 1. Flow around a small scale helicopter behind a wall in a windtunnel.

So the objective is to develop the formulation of the aerodynamic forces on a helicopter in non uniform flows. The ship or the frigate is only considered as a generator of a non uniform flow. The developments interest the formulation of the aerodynamic forces in any non uniform flow,

except that generally the frigate has an advance velocity. So we are concerned not only by hovering flight, but also by helicopters with an advance velocity close to the frigate velocity.

2. FORMULATION

The kinematics of the blades of a helicopter is the dynamic response of a flexible structure to aerodynamic and structural forces. The variations due to the non uniformity of the forward flow are difficult to simulate or to compute. To simulate as well as possible this kinematic on small scale helicopter with advance velocity, it is necessary to have a rotor head with control of the pitch angle of the blades, global and cyclic pitches.

The aerodynamic forces depend on the position and attitude of the rotor relative to the ship and also on the motor regime and the configuration of the ship: advance velocity, attitude and wind characteristics. Even where neglecting the unsteady effects, it is not possible to simulate all the configurations; so it is necessary to formulate the effects of the non uniform flow and to adjust some coefficients with some experiments and computations. The idea is to consider that the non uniform flow changes the local velocity field at the instantaneous location of the blade divided in strips. The global forces are obtained by a double integration during a complete rotation of the blade and along its span. The formulation steps are first to characterize the flow around the ship, to formulate the torque variation due to the non uniformity of the flow and then to adjust the coefficients on force and torque results.

For the experiments with the hypothesis of quasi-steady flight, the variations of the commands to get an equilibrium flight have to be measured: commands of pitch on the blades, of the power and of the tail rotor. On scale models equipped with radio control, the actual commands are not accessible due to gaps, absence of actuators and because the helicopter is fixed on the balance without a tail rotor. So the experiments consist on the measurement of the variations of the torque of the forces with a balance due to the non uniformity of the flow. For now it is expected to identify small variations of this torque.

3. PREVIOUS EXPERIMENTS

3.1. Helicopter scale model

The radio controlled helicopter was chosen with rotor head with global and cyclic control in pitch [3]. The rotor diameter has to be smaller than the deck width. The model chosen is the Sphynx 3D (Fig. 1): rotor radius R 360 mm, height 220 mm, fuselage length 720 mm, weight with battery included 0.85 kg. The rotor head is equipped with bell bars and small rods for the pitch control (Fig. 2 and 3). In flight its rotation rate is ~40 Hz. So the maximum velocity V at the blade tip is ~90 m/s and the minimum height ratio between the rotor and the floor is z/R=0.61. To simulate a ratio $\mu=2\pi\, n_{rot}R/V \approx 0.1$ between the tip velocity and the advance velocity, the wind tunnel velocity has to be low. n_{rot} is the rotation rate in revolution per second. After some tests the blades have been cut to get a diameter of 0.63 m such that the ratio between the rotor diameter and the deck width is ~0.6.



Figure 2. Helicopter Sphynx 3D.

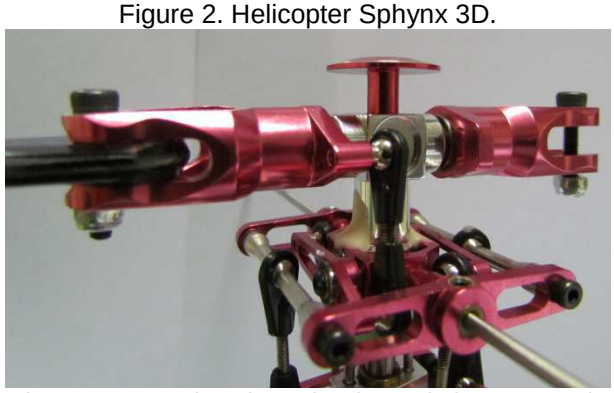


Figure 3. Rotor head mechanism, pitch commands and drag axis.



Figure 4. Complete head system.

3.2. Similarity

The blade tips flow is in the compressible regime for scale 1 helicopters. To simulate this regime it would be necessary to have a high rate rotation. The mechanical constraints at high regime are mechanically too important, so tests are only done in subsonic regime (~100 m/s). The Reynolds number is small; its maximum value at the blade tip is ~$2x10^5$. That is not too prejudicial if the maximum angles of the blade are relatively small, before any stall. The blades are not twisted as it would be necessary with an advance velocity. The blades have a NACA 0012 profile of 3 cm chord *c*. The rotor head on small scale helicopters are generally not equipped with a free flapping axis because the kinematic will not be similar with such a mechanism and the trim is controlled with the cyclic pitch. There is a drag axis (Fig. 2).

3.3. Vibrations

Small scale remote controlled helicopters are conceived for flying, but for the measurements of the forces torque, it is fastened on a balance. The control of the tail rotor has to be deactivated because the yaw moment cannot be compensated in adjusting its rotation rate. The interaction between the two rotors being moderated, it was decided to disconnect the tail rotor. The major problem encountered for these tests is the structural vibrations. The risk is to damage the balance during the transient phase of acceleration of the rotor. The first structural frequency is lower than the rotation rate of the rotor. So it is necessary to go quickly through the resonant regime. The structural damping on the fastened helicopter is so small that, without special care, emergency stops are necessary. To minimize the vibrations, dynamic balancing was realized [3] by adding small masses on a blade.

The power density spectrum of the thrust signal was measured by two techniques. In the first one, a micro electric motor with an unbalanced mass was activated on the rotor head; in the second the rotation rate of the rotor was modified. The power density spectrum between 1 and 80 Hz with the rotor in rotation and 200 Hz with the micro motor is presented on figure 4 with a value normalized to the one at 20 Hz. The first structural frequency is around 30 Hz and the second ~70 Hz.There is a lower frequency in static when the small rods are free to move.

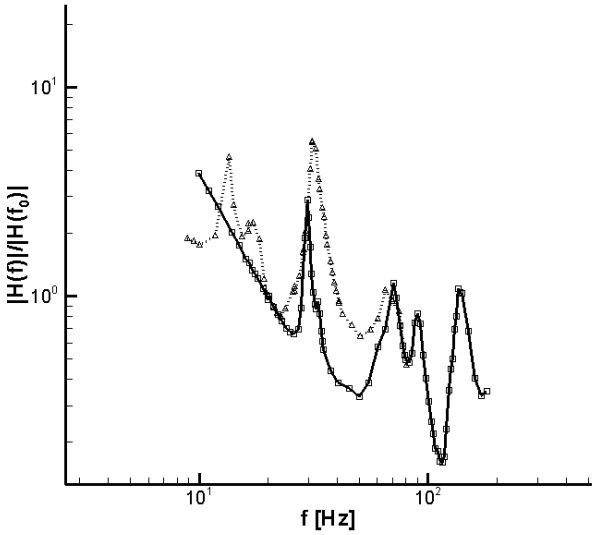


Figure 5. Thrust transfer funtion using a micro electric motor without rotation of the blades, (continued line), with the rotating rotor (dash line).

For the security of the balance, a pneumatic locking was developed (Fig. 5). Before starting and stopping the rotor, the balance is locked. After the starting phase, when the rotation rate is far from the resonance, the pneumatic jack is loosened. The inverse locking phase is done before the stop. Despite the mechanical locking system, there are mechanical shocks at the starts and stops.

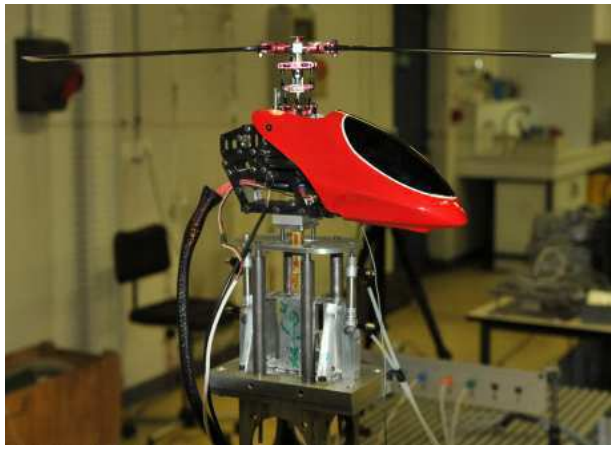


Figure 6. Pneumatic jack to jam the balance.

3.4. Wind tunnel tests

The helicopter without its fuselage is placed on a strut streamlined around the balance in the L2 wind tunnel (Fig. 6). It is a low velocity wind tunnel $V <$ 20 m/s. The distance between the floor and the helicopter is adjustable.



Figure 7. Helicopter in the L2 wind tunnel.

Measurements were done at different rotation rates in expecting to get the instantaneous forces during a blade rotation and after identification of the transfer function between the applied external forces and the balance signals. But the amplitude factor is so large at some frequencies that it is not possible to deconvoluate the signal and to get reliability on the external forces. Visualizations of the rotor head in rotation shows some elliptic deformations. So it was decided to continue the tests out of the wind tunnel until the balance gives correctly the aerodynamic forces.

4. EXPERIMENTS

With the batteries, the rotation rate of the rotor changes a little during the recording [3]; so they were replaced by a powerful electric supply at a fixed voltage. The rotor can then rotate until 65 Hz without too much warming and the acceleration to high rotation rate is very quick. The vibrations around the resonant frequency have not enough time to amplify. To eliminate some structural relatively high frequencies, the structural frame supporting the rotor head was reinforced; there is no constraint on the mass because the helicopter does not have to fly.

To validate the measurements, tests were first done in stationary flight. The longitudinal and lateral pitch angles are fixed in the neutral position. The radio control is deactivated. The global pitch is fixed mechanically with glue. In this configuration the blade kinematic has to be axisymetric and the aerodynamic forces have to be constant in time; the lateral forces and moments have to be null. There is only the secondary effect of the interaction between the blades and the fuselage that might induce periodic forces at the frequency $2.n_{rot}$ because there are two blades.

5. RESULTS

5.1. Signals analysis

Sampling at different acquisition frequencies and with different durations are analysed to verify that the rotation rate is well fixed and that the Fourier analyser gives reliable results. As the aerodynamic forces vary like the velocity to the square and that the structural vibrations are minimum around n_{rot} =50 Hz, the tests were done mainly around this frequency.

The six components of the balance are analysed by FFT (Fig. 7). For the six components of the balance the maximum of the Fourier coefficients are exactly at the same frequency. The signal of the rotor thrust is in clear blue and the rotor moment is in dark blue.

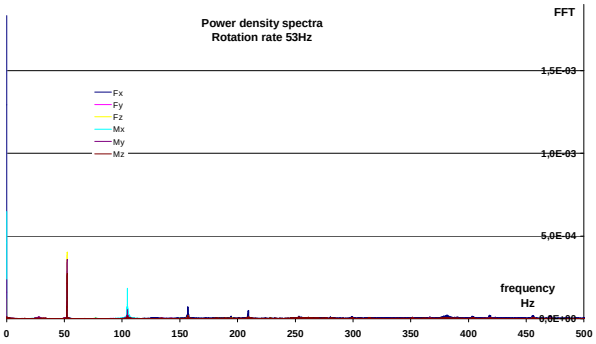


Figure 8. Power density spectrum of the six components balance.

The main signal comes from the mean value at frequency zero. Then the first spectrum line is in the lateral forces and moments at the rotation rate n_{rot}. The second spectrum line corresponds to the thrust and rotor moments at $2n_{rot}$; so there are relatively small variations of the aerodynamic forces on the two blades during a turn. It is not possible to measure accurately the variations of the aerodynamic forces during a 360° turn but the first Fourier coefficients can be identified.

5.2. Ground effect

To validate the measurements, tests are realised with a floor placed near the helicopter (Fig. 8). For stationary flight, the rotor plane is parallel to the floor and the ratio z/R of the rotor height to its radius varies from 0.6 to 2.7. The size of the floor $(4xR)^2$ can be considered as infinite, at a distance z/R=2.7 the floor has no effect. Some tests are also done with half the floor to simulate situation of helicopter recovery by the backward side of the deck. Other tests are realised with the rotor plane inclined with an angle θ relatively to the floor. To

simulate an advance velocity, an electric fan is placed behind the helicopter and the velocity of the longitudinal flow without rotation of the rotor is measured in different locations around the helicopter. The flow is not really uniform, but these tests are only preliminary to those in the wind tunnel.

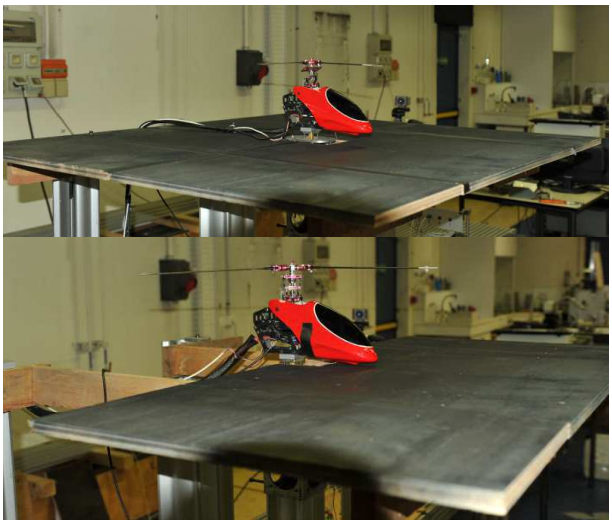


Figure 9. Floor set near the helicopter.

In hovering flight the ratio (Fig. 9) between the rotor thrust in ground effect T_{IGE} and the thrust out of ground effect T_{OGE} is similar to known results [1][8]. For different C_t = Thrust / ρ. A . Ω^2 R^2 thrust coefficients, the results are compared with a proposed formulation (1). In this formulation we have introduced empirical coefficients to take into account the value of C_t. The formulation gives large value of T_{IGE} /T_{OGE} for small values of z/R (< 0.5); but the height of any helicopter is generally larger than 0,6 R, so the formulation is not useful for z/R < 0,5. When only a part of the deck is under the helicopter, the ground effect can be characterized by the percentage of the deck under the area swept by the rotor. Globally the ground effect is proportional to this ratio. For the configuration of half-floor, the ground effect is half of the value for an unlimited floor see; point in orange (Fig. 9).

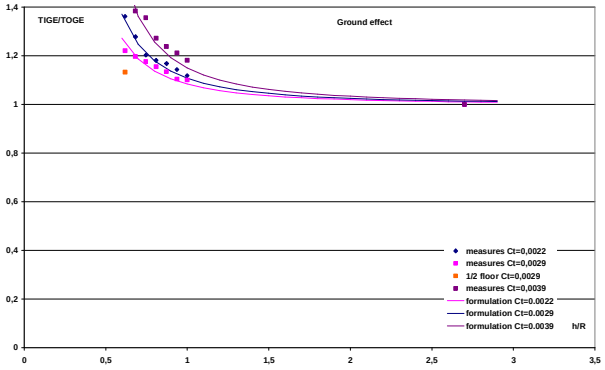


Figure 10. Formulation of the ground effect for different thrust coefficients.

$$\frac{T_{IGE}}{T_{OGE}} = \frac{1}{1-\left(\frac{z}{R}\right)^2 (49.C_T + 0.17)^2} \qquad (1)$$

For mechanical reasons it is necessary to move up the rotor before tilting it. Tests for z/R=0.89, μ =0.075 and n_{rot}=54 rps are presented in figure 10 with values reduced by the mean thrust without floor noted n° 1. The result 2 is with the floor, the results 3 to 6 are at an angle of 5.2°; without floor n° 3 the thrust does not depend on the angle θ. The effect of the floor is consequently reduced by the angle n° 4. The thrust is increased by the advance velocity n°5 and the ground effect with an angle θ and an advance velocity is relatively small.

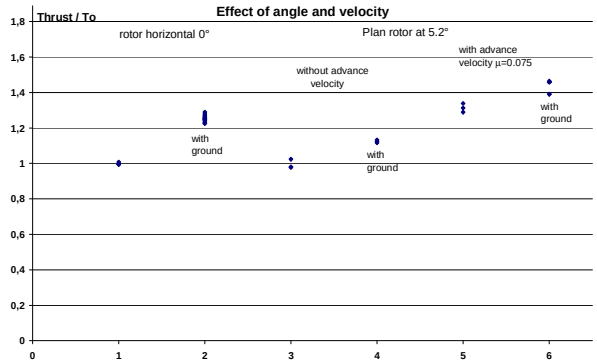


Figure 11.Thrust with and without floor, inclination and advance velocity.

6. VISUALIZATION

6.1. Photographs

The velocity of the rotor tip is ~100 m/s; if the shutter is of 1ms, the movement of the blade tip is of 0.1 m that is more than three times the blade chord *c*. To get unblurred images of the blade tip, the shutter has to be of about 20 μs. The energy of the light arriving on the CCD during this short duration is too low except if the white lighting is of hundred of watts and the CCD matrix is very sensitive. The most sensitive CCD with high resolution (4,256x2,832) is obtained with a reflex camera.

To materialize the flow, smoke is ejected at small velocity near the tip of the blade in front of the helicopter. In white lighting we only see the external volutes of smoke; so to visualize the flow, a 3 W laser sheet light up the vertical and symmetry plan in front of the helicopter. In this plan the flow velocities are smaller than 4 m/s and a shutter of 200 µs with a large optical aperture is satisfactory. The laser is in the green frequency (Fig.11). The reflected light on the front of the helicopter fuselage can be seen on the right

bottom side of this figure. As the depth of the field is very small, only the smoke in the lighted plan is correctly seen. The blade rotation generated some lateral velocities in this symmetry plane, so it seems that the smoke dense at some place disappears at another place. It fact the smoke is convected laterally in a zone unlighted. With image processing (Fig. 11) it is possible to improve a little the visualization of specific phenomena like the spreading of the smoke on the floor.

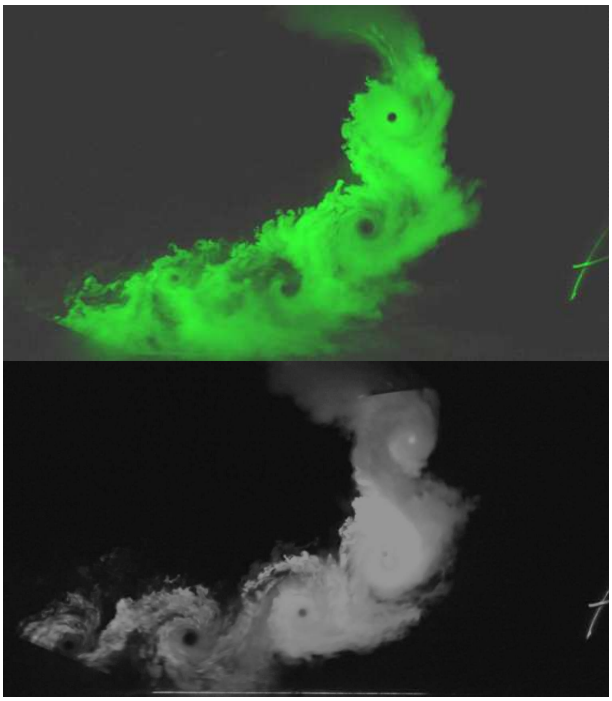


Figure 12. Photographs of the vortices shed at the tip blade.

6.2 Video

The same lighting technique is used with high rate video cameras. The image rate, which is linked to the shutter duration, is limited by the sensitivity of the CCD matrix or the lighting power. To see the evolution of small vortical structures it would be necessary that during the shutter opening its displacement is small relative to its size. For a convective velocity of the structure at ~2 m/s, the shutter has to be of 500 μs to get an accuracy of 1 mm: blurred images due to move. This is equivalent to a maximum rate frame of 2,000 i/s. It is not necessary to have a very high image resolution if the movement of the particles during the exposition represents several pixels.

Tests were done with high frame video camera photron APX-RS which has a resolution of $1{,}024^2$ pixels and a maximum transfer of the complete images at 6,000 i/s. Tests show that beyond 500 i/s the lighting is insufficient. A large volume rate of smoke is necessary to reflect the light so a smoke generator current in wind tunnel tests is used SAFEX (Nebelsonde NS2).

The films show that the vortices shed at the tip blades are nearly on a helix with small pith, the diameter decreases a little at the beginning and then the core of the vortices grows and their trajectory spread along the floor. Some snap shots are extracted of the films: figure 12 for a side view and figure 13 for a front view. In these figures the rotor plan is inclined at θ = -7° with respect to the floor. On the films, the background is black and the smoke is lighted in green; the helicopter and the blade do not appear. All the images are transformed by image processing in virtual colours and are superimposed on an image of the helicopter. As the rotor is rotating at a high speed, the blade is generally not in the lighted plane during the photography. On some images the trace of the blade tip marked in white appears; due to its deformation, it is not at the same location as when the rotor is turned off. So the blade position is artificially represented on the images in its rotating position.



Figure 13. Photograph extracted from films in virtual colours superimposed with an image of the helicopter and a blade, side view.

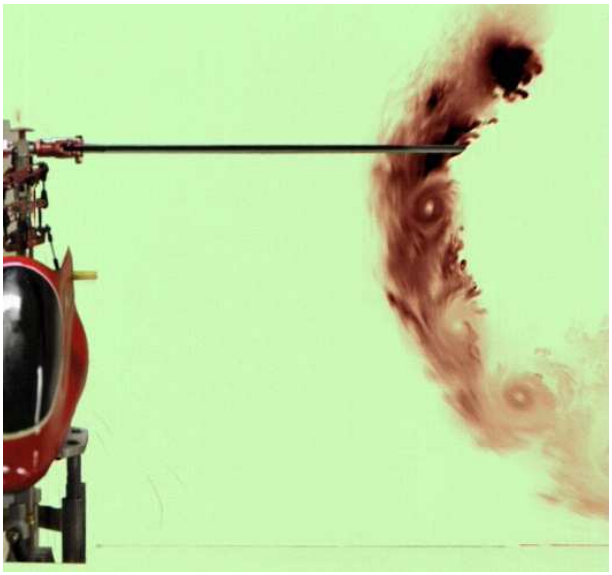


Figure 14. Front view of the shed vortices.

Some demonstration tests were realised with the new high rate video camera Redlake S7 which has a resolution of 1,920x1,080 pixels. Its sensitivity is larger than the other camera; so improved visualizations are obtained at 1,000 i/s (Fig. 14 & 15); the topology of the rotational flow is really more accurate. It appears an alternation of two tip blade vortices of different size and not equidistant.

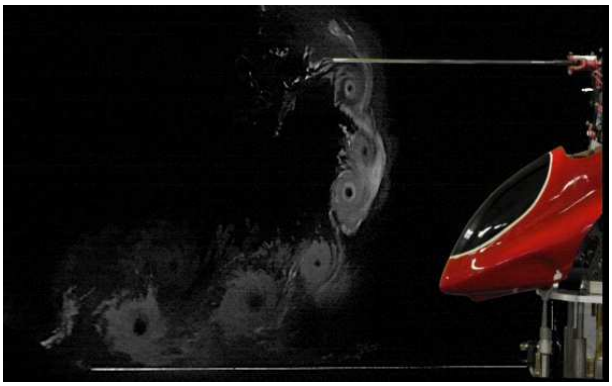


Figure 15. Tip blade vortices visualization with the new Redlake camera at 1,000 i/s.

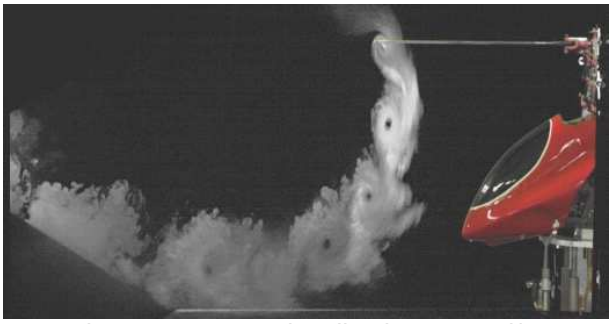


Figure 16. Same visualization at 500 i/s.

6.3 Image analysis

The films show that the evolutions of the vortices shed at the blade tip: trajectories, size of the vortex core and rotation of the vortices. All the images of some sequences of the films were extracted. On each image, the positions of the vortices are measured with a sub pixel accuracy, and then the successive positions of the vortex centre are reported in figure 16 for θ=0° and in figure 17 for θ= -7°. The vortices have the same trajectory except near the floor where there are interactions between them, with what looks like an alternation of upper and lower quasi-circular vortices along the floor.

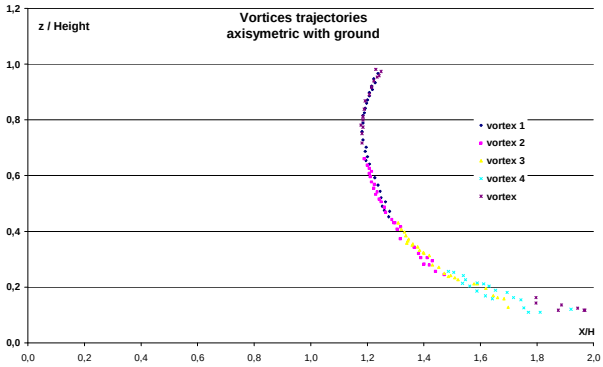


Figure 17. Trajectories of the vortices shed at the blade tip, rotor plane parallel to the floor θ =0°.

It is remarkable that the vortices are shed very close to the blade in height and at ~95 % in span. That does not correspond to the centre of gravity of the shed vortices resulting of a Prandtl scheme. The radius of the quasi-helicoïdal trajectories first decreases and then increases especially in the vicinity of the floor. When the rotor is inclined, the trajectories in front of the symmetry plane of the helicopter start nearer of the floor with a more important inside angle (Fig. 17). Even at θ = -7° and without advance velocity, the trajectories near the floor are still forward.

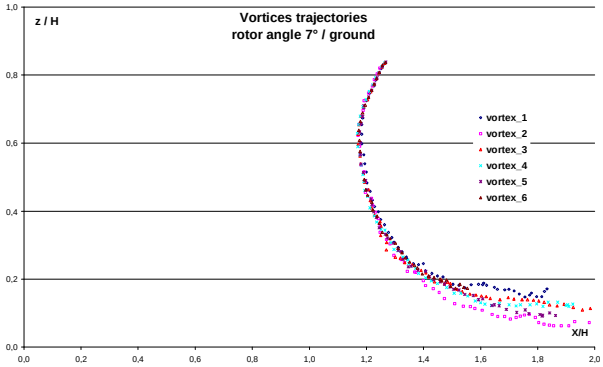


Figure 18. Trajectories of the vortices θ =7°.

Numerical derivations of the trajectories give estimations (Fig. 18) of the velocity components of the convection of the vortices. In the near wake these velocities accelerate until the radius of the helix is minimum and then they oscillate and decelerate progressively.

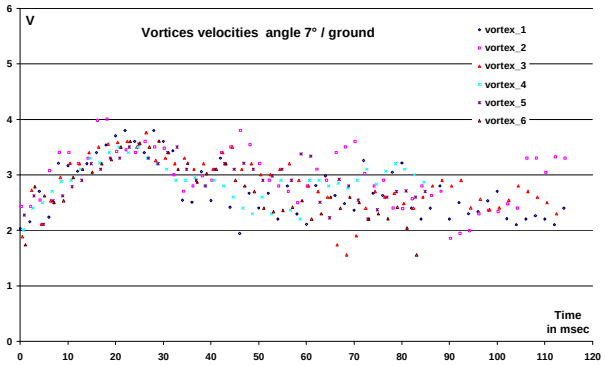


Figure 19. Velocity modulus obtained.

A code for an automatic tracking of the vortices was developed (Fig. 19). It is difficult to detect automatically some vortices on an image to initiate the tracking. The difficulty is that the current algorithms find the more probable position of a pattern defined on the first image. This does not work for any pattern size because the pattern near the vortex core changes and it turns. Other algorithms based on estimations of the rotation velocity for detecting some vortices do not work; if the threshold for vortex detection is too low, unrealistic vortices are wrongly detected. Other algorithms based on image autocorrelations by zones do not also work because the vortices warp. The detection of the trajectories in its bending zone is not efficient probably due to the variations of the vortices characteristics. It would perhaps be easier to analyse images of the flows without the floor.

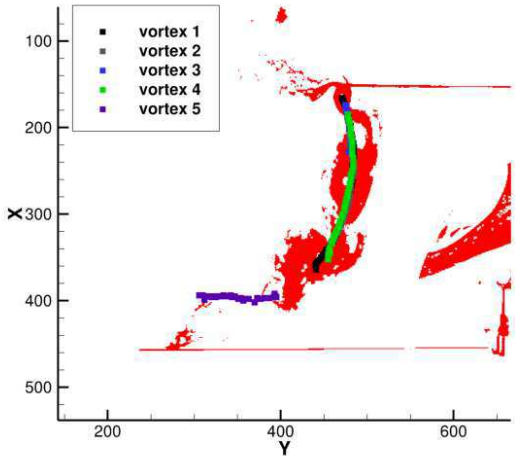


Figure 20. Automatic image analysis, some parts of the trajectories are detected.

7. PERSPECTIVES

If the aerodynamic angle of the blades is defined and that the flow regime does not change, the rotor thrust grows like $(n_{rot})^2$. The measurements of the thrust in function of n_{rot} are not consistent with this theory. During experiments it seems that the two blades have not the same trajectory. So high speed video films were realised with optical adjustments to visualize the crossings of the blade tips; large power light flood are used and the camera shutter is reduced to 20 μs. On some images taken at a rate of 3,000 i/s the blade tip is visible; its position and its angle can be measured. The result is that the two blade tips do not pass at the same height ($\Delta z \approx 0{,}2\ c$), the angles of the blade are not the same and they change with n_{rot}. So on the visualization, there are strong vortices generated by the up blade, and weak vortices generated by the low blade which are not equidistant between the two nearest vortices. So the tested conditions are not realistic for the aerodynamic of a helicopter and the results cannot be used for the formulation. So the perspectives are to build a new rotor head mechanism such that the pitch angle is identical on the two blades and well determined. First validation tests will be done in an axisymetric configuration and then all the other experiments will be done again.

8. CONCLUSION

The experiments with a small scale helicopter, which is available in stores of radio controlled models, show that the aerodynamic forces can be reliably measured. The ground effects can be identified. The vortices shed at the blades tip can be visualized; with some image processing their trajectories and their convection velocities can be measured in different observation planes.

Due to mechanical gaps in the rotor small rods which controlled the pitches, the results cannot be used, for now, to formulate the variations of the aerodynamic forces on a helicopter due to the non uniformity of the incoming flow. Modification of the rotor head mechanisms will be realized to access such formulation. It is also expected to get experimental results useful to validate numerical codes [10].

9. ACKNOWLEDGEMENT

Some results presented in the present communication have been supported by the International Campus for Safety and Intemodality in Transportation (www.cisit.org), the Nord Pas-de-Calais Region and the European Union.

10. REFERENCES

1. Bramwell A.R.S., Done G., Balmford D. (2001). Bramwell's helicopter Dynamics. *Butterworth Heinemenn IBSN 0 7506 5075.*

2. Herry B. (2010). *Etude aérodynamique d'une double marche descendante 3D appliquée à la sécurisation de l'appontage des hélicoptères sur les frégates.* Thèse Université Valenciennes.

3. Herry B., Bourez J.P. (2012). *Elaboration du programme d'essais et caractérisation du banc rotor L2 pour l'étude de l'interaction sillage rotor/sillage frégate*. Rapport technique Onera N° 5/18169 DAAP.

4. Herry B., Gardarein P., Rodriguez B., Van der Vorst J., Van Muijden J. (2011). *AT ROS-AIM Rotor-ship aerodynamic interface modelling- Model development.* Technical report Onera N° 5/16331 DAAP.

5. Keisbulck L., Labraga L., Paquet J.B. (2011). Flow bistability downstream of three-Dimensional Double Backward Steps at Zero-Degree Sideslip*. Journal of Fluids Engineering Vol. 133, n° 5.*

6. Herry B., Monnier J.C., Lamy M., Delva J., Verbeke C. (2011). *AT ROS-AIM Rotor-ship aerodynamic interface modelling- wind tunnel tests.* Technical report Onera N° 3-4/16331 DAAP.

7. Herry B.,Van der Vorst J. (2011). Towards the Impact of the Flow Bi-stability on the Launch and Recovery of Helicopters on Ships. 11th AIAA ATIO conference Virginia beach aerodynamics. Cambridge University Press.

8. Leishman J.G. (2006). *Principles of helicopter aerodynamics*. Cambridge University Press

9. Paquet J.B., Herry B. (2010). *AT ROS-AIM Rotor-ship aerodynamic interface modelling- bibliography and preliminaries investigations.* Technical report Onera N° 2/16331 DAAP.

10. Rodriguez, B. (2010). B. Blade Vortex Interaction & Vortex Ring State Captured by a Fully Time Arching unsteady Wake Model Coupled with a Comprehensive Dynamics Code. Heli Japan, Saitama (November 1-3).